

Characteristics and origin of lowermost stratospheric aerosol at northern midlatitudes under volcanically quiescent conditions based on CARIBIC observations

Bengt G. Martinsson,¹ Hung N. Nguyen,¹ Carl A. M. Brenninkmeijer,² Andreas Zahn,³ Jost Heintzenberg,⁴ Markus Hermann,⁴ and Peter F. J. van Velthoven⁵

Received 30 November 2004; revised 11 February 2005; accepted 25 March 2005; published 28 June 2005.

[1] Characteristics and origin of the aerosol in the lowermost stratosphere at northern midlatitudes were studied using measurements from a passenger aircraft (Civil Aircraft for Regular Investigation of the Atmosphere Based on an Instrument Container, or CARIBIC). Aerosol samples were collected during 60 intercontinental flights during 1999–2002 and analyzed for elemental composition with particle-induced X-ray emission (PIXE). Concurrent measurements of trace gases were used to interpret the aerosol measurements. It was found that particulate sulfur concentration increased steadily in the potential vorticity (PV) region of 2–7 PVU, whereas particulate potassium and iron showed no such dependence. The variability in concentration of the latter two elements was mainly connected with season, similar to their variation in the upper troposphere, whereas PV dominated the particulate sulfur variability. An ozone-based model was developed to quantitatively determine the mixing of stratospheric and tropospheric air masses. A significant dependence on PV was found, and the stratospheric fraction of the air peaked during spring. It was found that the particulate sulfur concentration was strongly dependent on the origin of the air masses. The concentration increased by a factor of 3 over the lowermost stratosphere. A discontinuity in the concentration over the tropopause indicated particle formation from sulfur dioxide transported across the tropopause. The concentration at the top of the lowermost stratosphere was used to estimate that the particulate sulfur production in the stratosphere is 0.066 Tg S/yr with approximately half of the amount transported across the top of the lowermost stratosphere originating in carbonyl sulfide.

Citation: Martinsson, B. G., H. N. Nguyen, C. A. M. Brenninkmeijer, A. Zahn, J. Heintzenberg, M. Hermann, and P. F. J. van Velthoven (2005), Characteristics and origin of lowermost stratospheric aerosol at northern midlatitudes under volcanically quiescent conditions based on CARIBIC observations, *J. Geophys. Res.*, 110, D12201, doi:10.1029/2004JD005644.

1. Introduction

[2] The lowermost stratosphere is bounded upward by the potential temperature at the tropical tropopause (380 K) and downward by the tropopause [Holton *et al.*, 1995]. It constitutes a significant fraction of the atmospheric column at midlatitudes, in the range of 15–20% in terms of mass. It is thus of similar size as the remaining, overlying stratosphere or the mixing layer of the planetary boundary layer. The properties of the aerosol in this large reservoir are poorly known in terms of chemical composition

and amount. Aerosol particles affect the radiation balance of the Earth by scattering of solar radiation and by changing the radiative properties of clouds [Intergovernmental Panel on Climate Change, 2001]. Stratospheric aerosol is involved in heterogeneous chemical reactions and the formation of polar stratospheric clouds, where rapid heterogeneous destruction of ozone occurs [Newman *et al.*, 2002].

[3] The presence of an aerosol layer in the stratosphere has been known for a long time [Junge *et al.*, 1961]. This aerosol mainly consists of sulfuric acid and water [Rosen, 1971; Arnold *et al.*, 1998]. Long-term measurements using balloon-borne instrumentation [Hofmann, 1993], satellite-based measurements [Kent *et al.*, 1995], and ground-based lidar measurements [Zuev *et al.*, 2001] demonstrate a highly variable aerosol load in the stratosphere, the variability of which is largely caused by explosive volcanic events. During the years from the early 1970s to present, there have been only a few periods without significant influence from volcanism, where stratospheric background conditions could be stud-

¹Division of Nuclear Physics, Lund University, Lund, Sweden.

²Division of Atmospheric Chemistry, Max Planck Institute for Chemistry, Mainz, Germany.

³Institute of Meteorology and Climate Research, Forschungszentrum Karlsruhe, Karlsruhe, Germany.

⁴Leibniz-Institute for Tropospheric Research, Leipzig, Germany.

⁵Royal Netherlands Meteorological Institute, De Bilt, Netherlands.

ied. The present study of the lowermost stratosphere over the years 1999–2002 spans such a period.

[4] The Brewer-Dobson circulation [Brewer, 1949; Dobson, 1956], a large-scale circulation of upward transport across the tropical tropopause, poleward transport in the stratosphere, and downward transport to the troposphere at midlatitudes and the polar regions, has a fundamental impact on the trace gases and aerosol in the lowermost stratosphere. This diabatic, downward transport brings down large quantities of ozone and sulfuric acid aerosol to the lowermost stratosphere. Both are formed by photochemical reactions initiated by energetic photons at higher altitudes.

[5] The lowermost stratosphere differs from the overlying, the so-called, stratospheric overworld [Hoskins, 1991] in the way that surfaces of equal potential temperature cross the tropopause and thus allow isentropic transport between the troposphere and the lowermost stratosphere [Dessler *et al.*, 1995]. A bidirectional transport across the extratropical tropopause was inferred from measurements of radioactive debris [Danielsen, 1968]. The magnitude of these cross-tropopause flows has been the topic of recent modeling efforts [James *et al.*, 2003; Sprenger and Wernli, 2003]. The transport from the troposphere to the lowermost stratosphere causes strong gradients for many chemical species above the tropopause. The concept of mixing lines for, e.g., ozone and carbon monoxide have been used to study this mixing [Hoor *et al.*, 2002; Zahn *et al.*, 2004a], but still no quantitative estimate of that process is available [Stohl *et al.*, 2003].

[6] Large quantities of sulfur dioxide and dimethyl sulfide are emitted from the Earth's surface. Chemical processing in the troposphere converts large fractions of these species to sulfate aerosol. Upward transport induces cloud formation in the moist troposphere, causing scavenging of a large fraction of the aerosol particles and water-soluble gases present. The formation of precipitation acts as a barrier to upward transport of these atmospheric constituents. The efficiency of this removal mechanism and its effects on the concentrations appearing in the upper troposphere are not understood quantitatively [Rasch *et al.*, 2000].

[7] Carbonyl sulfide (OCS) was proposed as a source of the stratospheric background aerosol [Crutzen, 1976]. OCS is the most abundant sulfur compound of the atmosphere. It is quite stable in the troposphere, but once transported into the stratosphere OCS is dissociated to finally form particulate sulfur. Recent measurements of particulate sulfur [Papaspriopoulos *et al.*, 2002] and sulfur dioxide [Thornton *et al.*, 1999] in the tropical middle troposphere as well as model results [Chin and Davies, 1995; Weisenstein *et al.*, 1997] indicate that these compounds contribute significantly to the particulate sulfur of the stratosphere. In addition, they can have a considerable effect on the stratospheric particle size distribution as a result of the high number concentration of aerosol particles observed in the vicinity of the tropical tropopause [Brock *et al.*, 1995].

[8] This work deals with the aerosol in the lowermost stratosphere. The concentrations of particulate sulfur, potassium, and iron were measured along with ultrafine particle size distributions [Hermann *et al.*, 2003] and a large number of trace gases [Zahn *et al.*, 2002] during

regular, intercontinental flights within the Civil Aircraft for Regular Investigation of the Atmosphere Based on an Instrument Container (CARIBIC) project [Brenninkmeijer *et al.*, 1999] (www.caribic-atmospheric.com) in the lowermost stratosphere at northern midlatitudes. The aim of this study was to explore the properties and origin of the aerosol. An ozone-based model was developed to quantify the mixing of air masses in the lowermost stratosphere and to estimate the particulate sulfur concentration at the lower and upper boundaries of the lowermost stratosphere. Furthermore, the contributions from precursors of the stratospheric particulate sulfur are inferred and production rates during background conditions are estimated.

2. Methods

[9] Sampling of aerosols and trace gases in the upper troposphere and lowermost stratosphere was undertaken from the CARIBIC platform, a Boeing 767-300 ER from LTU International Airways [Brenninkmeijer *et al.*, 1999]. The measurements presented here span a 3-year period from March 1999 to April 2002. The data set comprises observations from 60 intercontinental flights between Germany and destinations in the Indic (33 flights), South Africa (six flights), and the Caribbean (21 flights) (see Figure 1).

[10] Measurements were undertaken in the altitude range 8.2–12 km. A specially designed probe with separate inlets for trace gases and aerosols was placed 8 m from the nose of the aircraft and protruding 20 cm from the fuselage to prevent influence from the aircraft's boundary air layer. The aerosol inlet was of the diffuser type with an apex half-angle of 5°. Using wind tunnel experiments, the sampling efficiency of aerosol particles in the size range of interest here was estimated to be 90% [Hermann *et al.*, 2001].

[11] A dedicated aerosol sampler [Papaspriopoulos *et al.*, 1999] was used to collect aerosol particles in the diameter range 0.07–1.5 μm [Martinsson *et al.*, 2001], based on impaction technique. The sampler contained 14 sampling channels that were used to collect one integral sample covering the entire flight distance, and three to four samples in a time sequence (sequential samples) from each flight. The present study is based on the 205 sequential samples available. The sampling time was mostly 2.5 hours, extending down to 1 hour, which corresponds to flight distances of 2250 and 900 km. The samples were classified with respect to climate zones in the tropics (23°S–23°N), northern subtropics (23°N–37°N), and northern midlatitudes (37°N–64°N).

[12] The aerosol particles were collected on 0.2- μm polyimide films (API™), which were analyzed for elemental composition using particle-induced X-ray emission (PIXE) [Johansson and Campbell, 1988]. The analyses were undertaken at the Lund accelerator facilities, using 2.55-MeV protons. X-rays were detected at 135° using a lithium-drifted silicon detector from Kevex™ and a high-purity germanium detector from Canberra™. The proton beam current was 60 nA, and the accumulated beam charge per sample was 80 μC . The setup was calibrated with thin standards from Micro-Matter™, and the resulting inaccuracy in the elemental analysis was 10%. Further details about the

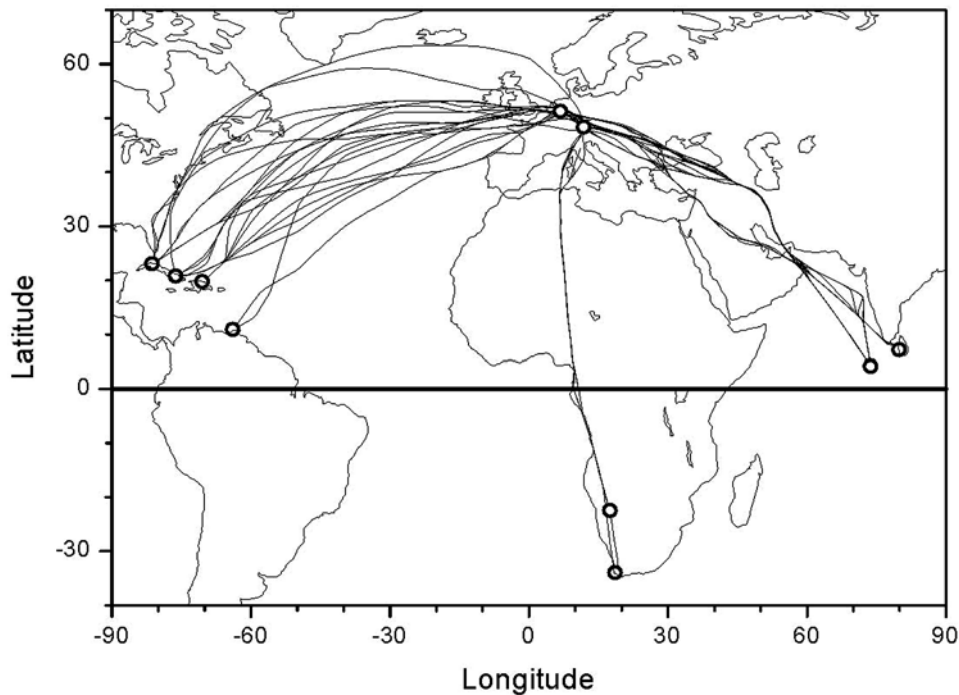


Figure 1. The 1999–2002 flight tracks of CARIBIC. Flights were carried out between Germany and the Indic (33 flights), South Africa (six flights), and the Caribbean (21 flights).

analysis as well as the handling of the detection limit are given by *Papaspiropoulos et al.* [2002]. The analytical results are presented as mass concentration normalized to STP (standard pressure (1013 hPa) and temperature (273 K)).

[13] A large number of trace gases are measured from the CARIBIC platform. In the present study the O_3 measurements were used. O_3 was measured with a time resolution of 17 s with a method based on UV absorption. Data averaged over 2–3 min were used here. The uncertainty is estimated to the greatest of 4% and 4 ppbv [*Zahn et al.*, 2002].

[14] The identification of samples taken in the stratosphere was based on the dynamical tropopause. Typical threshold values of the potential vorticity (PV) are in the range of 1.5–3.5 PVU (potential vorticity unit; $1 \text{ PVU} = 10^{-6} \text{ K m}^2 \text{ kg}^{-1} \text{ s}^{-1}$) [*Hoerling et al.*, 1991; *Hoinka*, 1997]. PV was calculated from archived European Centre for Medium-Range Weather Forecasts (ECMWF) analyses with a resolution of 1×1 degree in the horizontal and 31 (1999–2001) to 60 (2001 to present) vertical hybrid sigma-pressure model levels. The PV values were interpolated linearly in longitude, latitude, log pressure, and time to the position of the aircraft. Five-day back-trajectories were calculated from the position of the aircraft every second minute. Figure 2 shows the relation between the 5-day average PV along the trajectories and the PV at the position of the aircraft. In most cases they agree well, implying that the PV at the aircraft position well represents the PV in the air mass over the last 5 days. On the basis of PV at the aircraft position, the aerosol samples in a first step were classified with respect to whether air from the lowermost stratosphere was sampled. In a refined analysis, the samples identified from the PV-based evaluation were further analyzed regarding the origin of the air sampled in the lowermost stratosphere, based on

the O_3 concentration. This will be described in detail in section 4 and Appendix A.

3. Results

[15] The CARIBIC sampling flights (Figure 1) most of the time covered northern midlatitudes, the subtropics, and the tropics and only occasionally reached the subtropics of the Southern Hemisphere. Figure 3 shows the particulate sulfur concentration in relation to the sample average PV along the flight track for all the sequential samples. It can be seen that most of the samples (74%) were taken at average

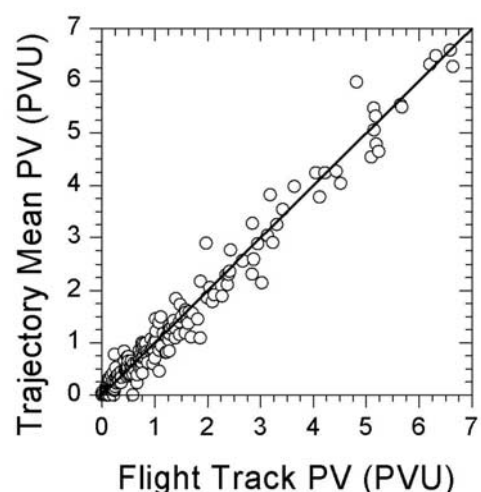


Figure 2. Average potential vorticity along 5-day backward trajectories related to the potential vorticity along the flight track.

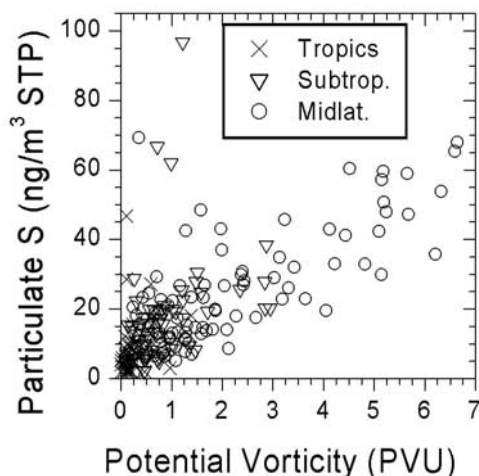


Figure 3. Particulate sulfur concentration as a function of the potential vorticity.

PV of below 1.5 PVU, indicating that they were mainly representative of tropospheric air. At PVs larger than 3 PVU only samples from midlatitudes are found. This observation is consistent with the fact that the tropopause height decreases with increasing latitude and that the sampling was undertaken at fairly constant altitude. A few samples from the subtropics were taken at average PVs up to almost 3 PVU. It can be seen that they generally agree with the particulate sulfur concentration at midlatitudes. However, given the small amount of data available from the tropics and subtropics, this study of the lowermost stratosphere is confined to northern midlatitudes.

[16] Although PIXE is a multielemental analytical technique, the present study is limited to three elements, sulfur, potassium, and iron, because the small amount of sampled particulate mass causes problems with the detection limit [Papaspriopoulos *et al.*, 2002]. Figure 4 shows the concentration of the three elements as a function of the sample average PV along the flight track. The measurements were subdivided into five PV groups (0–1, 1–1.5, 1.5–2.5, 2.5–5, and >5 PVU) in order to analyze the PV dependence of the concentration. The average concentrations are depicted as filled diamonds at the average PV of each group together with the standard deviation of the average. For two of the elements, potassium and iron, the PV dependence is small compared with the overall variability of the data. No trend deviating from the average concentrations of 0.50 and 0.59 ng/m^3 STP over all PVs (dotted lines) can be identified for potassium and iron.

[17] The particulate sulfur concentrations were analyzed in the same way as potassium and iron. In Figure 4 it can be

seen that the concentrations in the two lowest PV categories are similar. For PVs larger than 1.5 PVU the particulate sulfur concentration steadily increases with PV. This average behavior was approximated with two linear segments

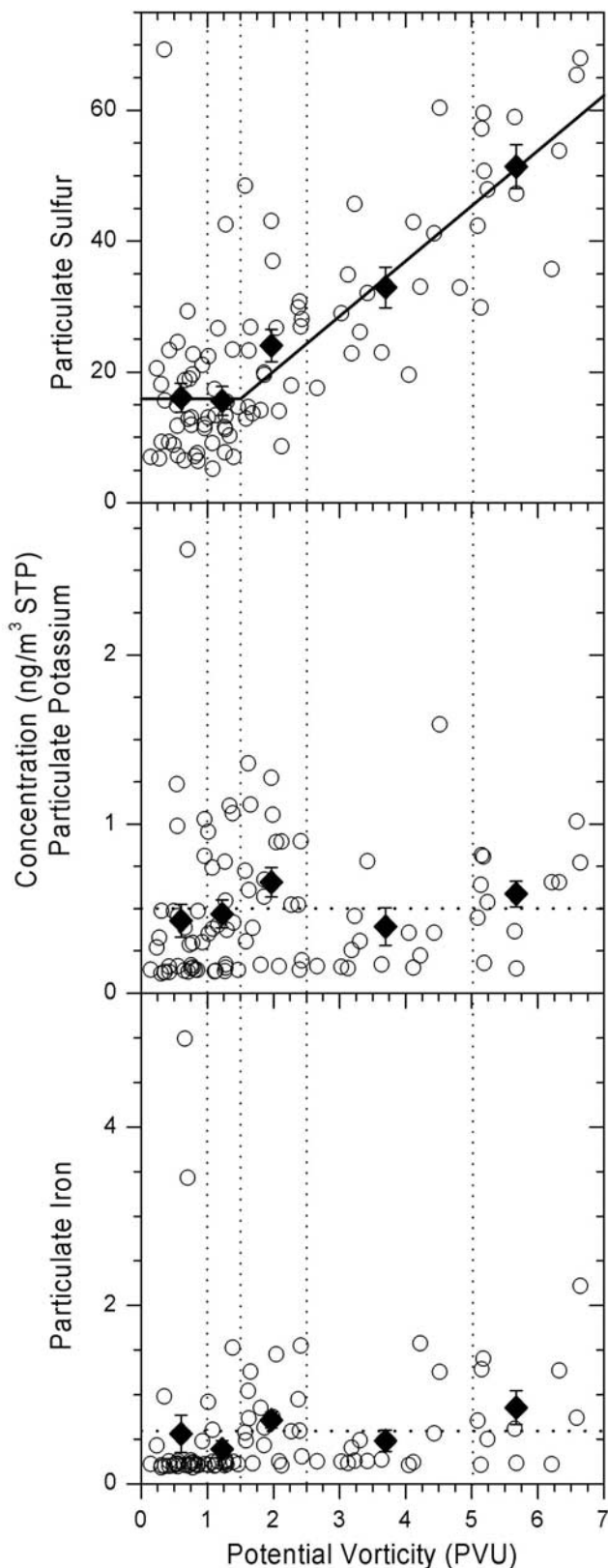


Figure 4. Aerosol elemental concentration at northern midlatitudes as a function of the average potential vorticity. Circles represent the measurements. The diamonds give averages and their standard deviations over the PV regions marked by the vertical dotted lines. The dotted horizontal lines show the average concentrations of potassium and iron, whereas the bold line of the sulfur graph consists of two linear fits to the data.

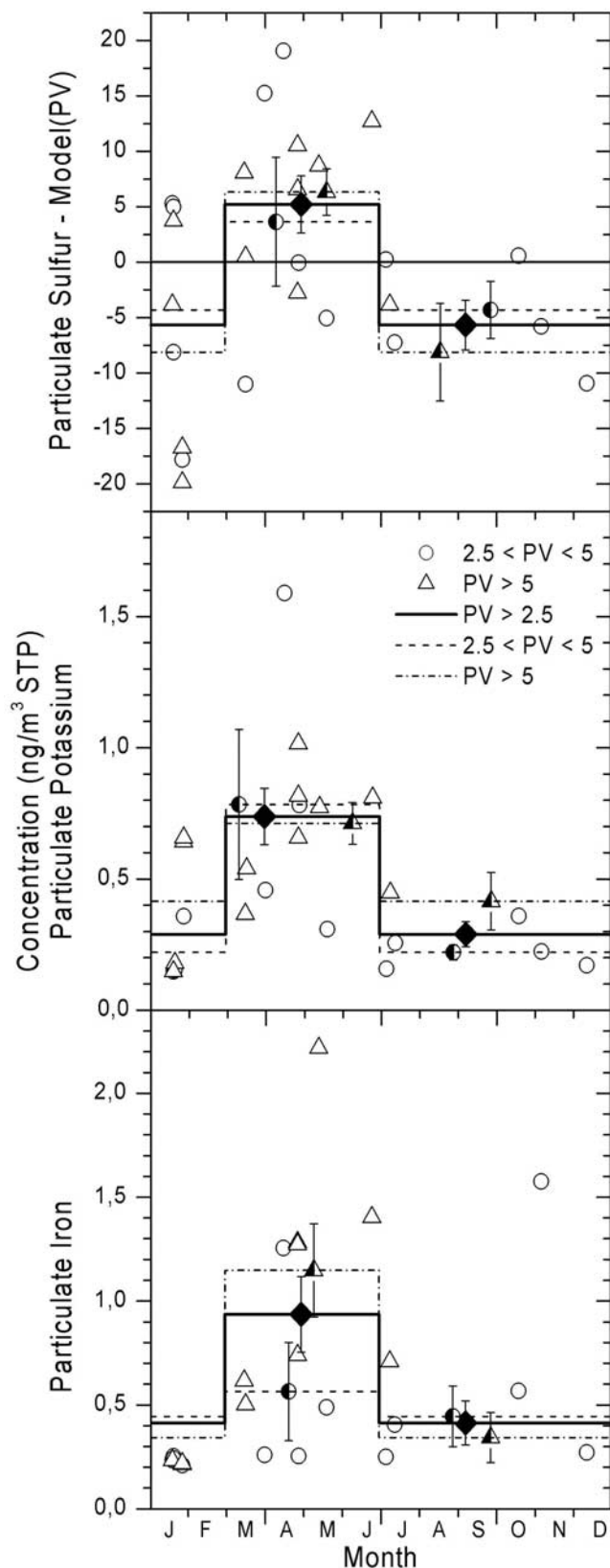


Figure 5. Aerosol elemental concentration at northern midlatitudes as a function of season for samples of average potential vorticity of more than 2.5 PVU. The particulate sulfur concentrations are given as difference between the original value and the linear model of Figure 4.

(the bold, solid line of Figure 4). In the PV range 0–1.5 PVU the average particulate sulfur concentration is $15.9 \text{ ng/m}^3 \text{ STP}$. This can be regarded as an estimate of the concentration in the upper troposphere at northern midlatitudes, using 1.5 PVU as the dynamical tropopause. At higher PVs, air from the lowermost stratosphere is sampled, and the concentration increases steadily with PV and reaches on average $62 \text{ ng/m}^3 \text{ STP}$ at 7 PVU.

[18] The focus of this study is the aerosol in the lowermost stratosphere. Therefore the attention in the forthcoming analysis is limited to samples that to a large degree, were taken in the lowermost stratosphere. The limit was set to samples with the average PV of 2.5 PVU. In total, 26 samples were taken in air with the average PV above that limit.

[19] The concentrations of the elements in Figure 4 vary significantly around their average. One factor behind this behavior could be a seasonal variation. For potassium and iron the slope of the average concentration as a function of PV is zero. This means that the measured concentrations can be used without any conversion to study the seasonal variation. The particulate sulfur concentration depends strongly on PV. To study the seasonal dependence of this element, we subtracted the PV-dependent average concentration from the actually measured concentrations. The data were analyzed separately in two PV groups, 2.5–5 and >5 PVU. With the limited amount of lowermost stratospheric data available, the year was divided into two seasons, the spring (March–June) and the remainder of the year, with approximately the same number of samples. In Figure 5 it can be seen that the three elements are present in significantly higher concentrations during spring compared with the remainder of the year. It can also be seen that this pattern holds in both PV groups, with the exception of iron in the 2.5–5 PVU group.

[20] By comparing Figures 4 and 5 with respect to the concentration of particulate potassium and iron, it can be concluded that the season is more important than the PV level, i.e., how deep into the lowermost stratosphere the sample was taken. The seasonal pattern of a strong peak in concentration during spring coincides with the peak concentration in the upper troposphere [Papapiropoulos *et al.*, 2002]. This indicates that the potassium and iron originate in the troposphere and reach the lowermost stratosphere as a result of transport across the tropopause.

[21] The particulate sulfur concentration peaks in the same month as the other two elements studied. However, whereas the average concentration increases by $46 \text{ ng/m}^3 \text{ STP}$ in the PV interval 1.5–7 PVU, the seasonal variation accounts for approximately $\pm 5 \text{ ng/m}^3 \text{ STP}$. This increasing particulate sulfur concentration as the measurements are taken deeper into the lowermost stratosphere will be investigated further in the next section, using the O_3 concentration measurements.

4. Origin of Air and Particulate Sulfur in the Lowermost Stratosphere

[22] To put the results from the lowermost stratosphere further into a dynamic context, the fraction of the air originating in the stratospheric overworld (f_{SOV}), i.e., above the 380-K potential temperature surface, was estimated for

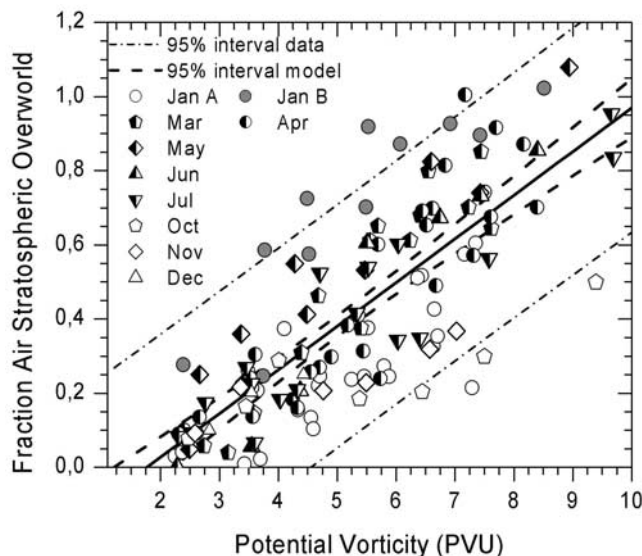


Figure 6. The fraction of the air that originated in the stratospheric overworld as a function of the potential vorticity for each sample and their PV levels as defined in the text. The January measurements are divided into two categories: those from the year 2000 (Jan B) and those from 2001 and 2002 (Jan A). The solid line is a linear fit, the dashed lines are the 95% confidence interval of the model, and the dash-dotted lines are the 95% confidence interval of the data points.

each sample. This quantity can in principle be obtained from modeling of the fluxes to, from, and within the lowermost stratosphere. However, there are still large uncertainties associated with these fluxes. Therefore the long-lived O_3 [Solomon *et al.*, 1997; Smith *et al.*, 2001], which is produced higher up in the stratosphere, was used as a tracer together with only simple, overall assumptions about the air fluxes to obtain an estimate of f_{SOV} . The model used to compute f_{SOV} is presented in the Appendix A. Appendix A also contains a sensitivity study showing that the model is a robust tool for estimation of the fraction of the air and particulate sulfur of stratospheric origin.

[23] The 26 CARIBIC measurements investigated here, covering 1–2.5 hours of aerosol sampling time, were broken down into eight PV levels, one with tropospheric air having PV less than 2 PVU, one with PV > 8 PVU, and six layers of 1 PVU width between 2 and 8 PVU. The PV, O_3 concentration, and latitude were averaged in each PV layer for each of the 26 sampling occasions. The seven stratospheric layers were used to estimate the fraction of air from the stratospheric overworld (f_{SOV}) sampled in each of the layers by relating the measured average O_3 concentration of each layer to the O_3 concentrations at the two boundaries of the lowermost stratosphere, as obtained from the model. For the entire time period of an aerosol sample, f_{SOV} was obtained as the product of the time spent in each layer and f_{SOV} of the layers divided by the entire sampling time.

4.1. Seasonal Variation in Air Origin

[24] The atmosphere has a strong gradient in PV in the tropopause region, which is used to define the dynamical

tropopause. Tropospheric air enters the lowermost stratosphere as a result of transport across the tropopause. The gradient in PV thus could also be expected to cause a gradient in f_{SOV} . Figure 6 shows the relation between f_{SOV} and PV for the PV layers of the samples. Overall, it can be seen that f_{SOV} varies substantially for a given PV and that the average f_{SOV} increases steadily with PV. (The linear model in Figure 6 is used in the sensitivity study described in Appendix A.)

[25] A clear seasonal variation in the dependence of f_{SOV} on PV can be seen. The measurements taken in October–December were more affected by tropospheric air than those from March–July. It is also clear that the measurements from January show large variability. Mostly they behave similar to the October–December measurements (Jan A), but they can also appear at the other extreme (Jan B) in Figure 6. The January data were obtained from eight sampling events. Those marked Jan B were the results from two of these events. They were sampled 18 and 19 January 2000. The other six events were from 2001 and 2002. Clearly, observations of the strong winter/spring downward transport from the stratospheric overworld were made already in January of the year 2000. The remaining January events are less influenced by air from the stratospheric overworld.

[26] The seasonal pattern thus consists of a strong influence of air from the stratospheric overworld on the lowermost stratosphere during late winter, spring, and early summer, which in some years can be observed already in January. Later in the year, influence from the overworld fades, and thus the fraction of the air originating in the troposphere is larger during fall and early winter. A similar seasonal behavior was obtained by studying the O_3 gradient with PV (dO_3/dPV), yielding a maximum in April and a minimum in October [Roelofs and Lelieveld, 2000; Zahn *et al.*, 2004b]. However, dO_3/dPV is not directly comparable with f_{SOV} because the seasonal variability of the former is the combined effect of the seasonal variability of the O_3 concentration at the top of the lowermost stratosphere and mixing with tropospheric air in the lowermost stratosphere.

4.2. Particulate Sulfur Dependence on Air Origin

[27] In Figure 6 the data from the different PV levels of each sampling occasion were used. As we now turn the attention to particulate sulfur, the results from the PV levels of each sample are combined to describe f_{SOV} of the entire sampling period. This quantity should be compared with the particulate sulfur concentration reduced for the impact from the troposphere ($C_{S, strat}$), i.e.,

$$C_{S, strat} = C_{S, meas} - (1 - f_{SOV})C_{S, troposph}, \quad (1)$$

where the concentration and seasonal variation of upper tropospheric particulate sulfur was obtained from the CARIBIC data set. The results are shown in Figure 7. The particulate sulfur concentration increases with f_{SOV} . A linear model was fitted to the $C_{S, strat} - f_{SOV}$ relation, using a forecasting method. The dash-dotted lines indicate on the 95% probability level that a measurement will appear within these borders. The bold dashed lines relate to the linear model and show the limits where the line is contained with 95% probability. In Figure 7 it can be seen that the

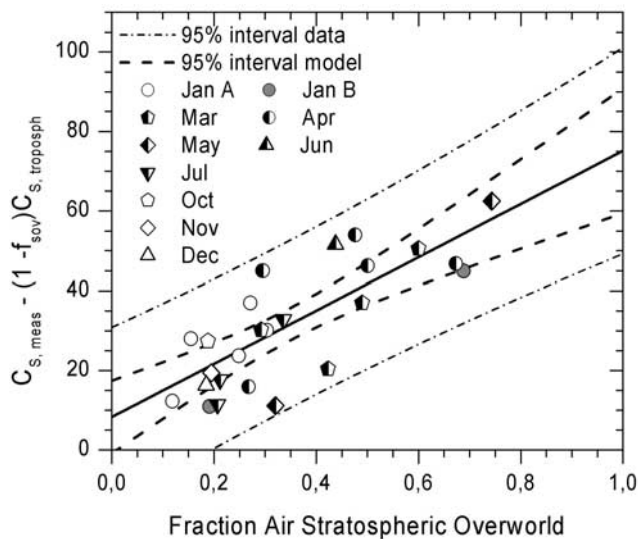


Figure 7. Measured particulate sulfur concentration at northern midlatitudes reduced by the estimated contribution from the troposphere as a function of the fraction of the air that originated in the stratospheric overworld. Jan B and Jan A samples were taken in January 2000 and 2001–2002, respectively. The solid line is a linear fit, the dashed lines are the 95% confidence interval of the model, and the dash-dotted lines are the 95% confidence interval of the data points.

variability relative to the linear model cannot be assigned to season. The samples with the largest f_{SOV} were, with the exception of one of the January 2000 measurements, taken during spring, thus concurring with the finding of Figure 6 that f_{SOV} is larger during these months. The seasonality of the transport from the overworld thus provides an explanation for the seasonal dependence of the particulate sulfur concentration in the lowermost stratosphere (Figure 5).

5. Discussion

[28] The tropospheric component was removed for the particulate sulfur concentrations of Figure 7 ($C_{S, strat}$). Restoration of C_S to the total concentration is obtained by

$$C_S = C_{S, strat}(f_{SOV}) + (1 - f_{SOV})C_{S, troposph}. \quad (2)$$

[29] The average upper tropospheric concentration at northern midlatitudes was 15.9 ng/m^3 STP. In Figure 7 it can be seen that $C_{S, strat}(0) = 8.3 \text{ ng/m}^3$ STP, according to the linear model. This value is larger than zero with a high probability (approximately 97%). The tropopause thus likely produces a discontinuity in the particulate sulfur concentration, being 16 ng/m^3 STP in the tropospheric limit and 24 ng/m^3 STP in the stratospheric limit of the tropopause. The cause of this discontinuity could be transformation of sulfur dioxide that is transported along with particulate sulfur across the tropopause, as proposed by Papaspiropoulos *et al.* [2002]. At the top of the lowermost stratosphere, at atmospheric pressure of typically 138 hPa (130–145 hPa depending on latitude), the particulate sulfur concentration becomes $C_{S, strat}(1)$, namely, 75 ng/m^3 STP. The results are summarized in Figure 8.

[30] Deshler *et al.* [2003] compared three data sets in two altitude intervals based on balloon-borne instrumentation at Laramie (41°N), Wyoming, and Lauder (45°S), New Zealand [Liley *et al.*, 2001], and satellite-based measurements from SAGE II [Bauman *et al.*, 2003]. During the time period of the present measurements, spring 1999 to spring 2002, the total aerosol volume columns according to these measurements were 1.5×10^4 and $2 \times 10^4 \mu\text{m}^3/\text{cm}^2$ for the 5-km intervals 20–25 km and 15–20 km. Making the assumptions that the aerosol consists of 75% sulfuric acid and 25% water [Rosen, 1971] and that the column concentrations are representative of the middle pressure of the altitude intervals, the total aerosol volume columns transforms to 200 and 130 ng/m^3 STP of particulate sulfur at 50 and 98 hPa atmospheric pressure.

[31] The balloon-borne and satellite-based measurements cannot directly be compared with the results from the CARIBIC platform, because they are from different altitudes and because the former measurements are not chemically specific. However, a linear extrapolation of the results from the stratospheric overworld to the top of the lowermost stratosphere (the dashed line of Figure 8) results in a similar concentration as obtained from CARIBIC, thus suggesting that the data sets are in coherence.

[32] The results of this study were obtained for a period where the influence from volcanism on stratospheric sulfur was small, and are thus representative of what is often referred to as stratospheric background conditions. In the same way as meridional mixing of O_3 -poor tropical air with the down-welling air from the production altitudes causes a strong vertical gradient in the O_3 concentration [Gettelman *et al.*, 1997], such a mixing of the particulate sulfur produced from carbonyl sulfide (OCS) explains the profile

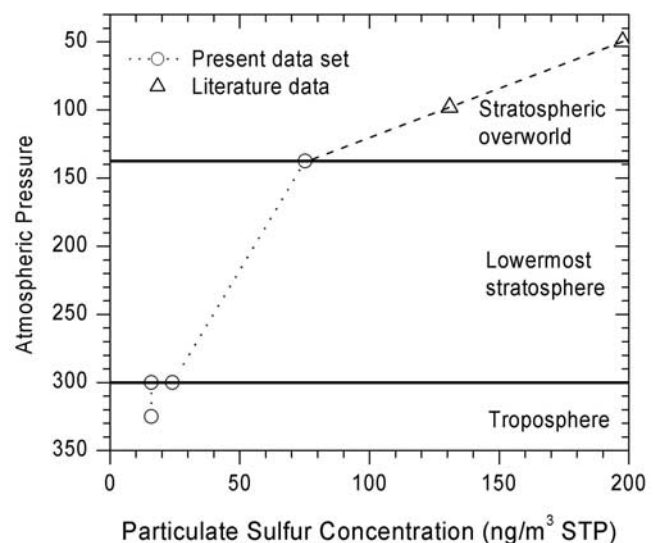


Figure 8. Particulate sulfur concentration at northern midlatitudes for various atmospheric pressures. The circles are from the present data set, and the triangles represent literature data from Deshler *et al.* [2003]. The latter data were given as particle volume in 5 km altitude columns. They were converted to particulate sulfur mass concentrations assuming the particle composition to be 75% sulfuric acid and 25% water. See the text for further details.

of particulate sulfur in the extratropical stratosphere. In the lowermost stratosphere, mixing with tropospheric air caused by transport across the tropopause further reduces the particulate sulfur concentration. At low altitudes, in the planetary boundary layer (PBL), the particulate sulfur concentration is high as a result of oxidation of sulfur dioxide and dimethyl sulfide and primary particle emissions from surface sources. Vertical transport of particulate matter in the troposphere is suppressed by wet scavenging. Thus mixing dilutes the stratospheric source and wet scavenging removes particles from the surface sources to create a minimum in the STP mass concentration of particulate sulfur in the upper troposphere at midlatitudes.

[33] *Bauman et al.* [2003] estimated the effective diameter of the aerosol to 0.3 μm during volcanically quiescent periods. The standard deviation of their lognormal distribution was estimated 1.6, implying that 90% of the mass was carried by particles less than 0.6 μm in diameter. With the particle composition according to *Rosen* [1971], the sedimentation velocity becomes 0.15 km/month for the latter particle size and the conditions in the lowermost stratosphere. The vertical extension of the lowermost stratosphere at midlatitudes is several kilometers. Comparing these numbers with the estimated air residence time of 2.5–6 months (see Appendix A) in the lowermost stratosphere indicates that transport across the tropopause along isentropic surfaces into the troposphere is the main removal mechanism of particulate sulfur from the lowermost stratosphere at midlatitudes.

[34] On the basis of budgetary considerations, *Chin and Davies* [1995] questioned the dominance of the OCS source for background conditions. Sulfur dioxide injected to the stratosphere is converted to particulate sulfur at lower altitudes than OCS. As already pointed out, deposition processes of particulate sulfur in the stratosphere are weak. Therefore it is possible to estimate the strength of sources to the aerosol based on concentrations appearing at key locations. Ideally the concentration of particulate sulfur and sulfur dioxide at the tropical tropopause should be available. The concentration measurements available from 8–12 km altitude will be used as a substitute to estimate that concentration. After processing of OCS in the stratosphere and mixing with tropical, stratospheric air, the particulate sulfur concentration at the top of the lowermost stratosphere represents the sum of the tropospheric contributions of particulate sulfur (9 ng/m^3 STP [*Papaspiropoulos et al.*, 2002]) and sulfur dioxide (30 ng/m^3 STP [*Thornton et al.*, 1999]) and the aerosol produced from OCS. The concentration at northern midlatitudes was estimated to 75 ng/m^3 STP in the present study. These numbers thus indicate that OCS is responsible for approximately half of the particulate sulfur mass that is transported down to the lowermost stratosphere.

[35] The stratospheric aerosol concentrations are similar at southern and northern midlatitudes [*Deshler et al.*, 2003]. Taking the present estimate of the particulate sulfur concentration at the top of the lowermost stratosphere to be representative of the extratropics and using the flux across the 380-K potential temperature by *Appenzeller et al.* [1996] results in a production of 0.032 Tg S/yr from OCS, whereas the flux of particulate sulfur and sulfur dioxide from the tropical troposphere to the stratosphere becomes

0.034 Tg S/yr. The estimate of the production from OCS is somewhat lower than that from *Chin and Davies* [1995] of 0.052 Tg S/yr. Other recent estimates on the production of the stratospheric background aerosol are 0.049 and 0.011 Tg S/yr [*Weisenstein et al.*, 1997], 0.013 and 0.178 Tg S/yr [*Kjellström*, 1998], and 0.036 and 0.031 Tg S/yr [*Takigawa et al.*, 2002] from OCS and sulfur dioxide, respectively, transported from the troposphere. Clearly, further efforts are needed to better quantify the sources of the stratospheric background aerosol.

6. Conclusions

[36] Regular measurements of particulate sulfur and other elements of the aerosol in the upper troposphere and the lowermost stratosphere (8.2–12 km altitude) were undertaken from the CARIBIC platform during 1999–2002. During this time period the volcanic influence on the stratospheric aerosol was low. The focus of this study was the aerosol of the lowermost stratosphere at northern midlatitudes under these volcanically quiescent conditions.

[37] Three chemical elements were investigated in relation to the potential vorticity (PV) of the air mass, which has a strong gradient of increase from the tropopause. Particulate potassium and iron showed no measurable change in concentration as PV increased. Particulate sulfur, on the other hand, strongly increased from the average concentration of 16 ng/m^3 STP (standard temperature and pressure) in the upper troposphere to 62 ng/m^3 STP at the PV of 7 PVU. The samples taken in stratospheric air masses having PV > 2.5 PVU were investigated with respect to seasonal variation. Particulate potassium and iron strongly peaked in concentration during March–June, which is similar to their seasonal behavior in the upper troposphere. Particulate sulfur concentration peaked during the same months, but not as pronounced as the other two elements. Combining the results of the PV and seasonal dependences, it can be concluded that particulate potassium and iron in the lowermost stratosphere originate in the troposphere and appear as a result of transport across the tropopause, whereas particulate sulfur has a strong stratospheric source in addition to the transport across the tropopause.

[38] The problem of quantifying the mixing in the lowermost stratosphere is still unsolved. Here a solution to the problem is proposed, based on a tracer technique. A model was developed to estimate the fraction of the intercepted lowermost stratospheric air masses that originated in the stratospheric overworld (f_{SOV}). The model was in its essential parts based on ozone (O_3) as tracer, due to its long chemical lifetime in the lowermost stratosphere, and availability of O_3 measurements concurrent with the aerosol measurements from the CARIBIC platform as well as ozonesonde measurements of the concentration at the top of the lowermost stratosphere and in situ measurements in the upper troposphere. The concentrations at the top of the lowermost stratosphere and the upper troposphere were integrated in time using estimated values of the chemical lifetime and the residence time of air in the lowermost stratosphere, to obtain the O_3 concentrations from the two boundaries affecting the lowermost stratosphere at any given time. These concentrations from the boundaries were then applied to the O_3 measurements in the lowermost

stratosphere to obtain the estimate of f_{SOV} . A sensitivity study showed that this model produced robust estimates of the fraction of the lowermost stratosphere air that had passed through its upper boundary.

[39] The relation between f_{SOV} and PV showed a strong seasonal variation in the lowermost stratosphere, with the strongest influence from the overworld during late winter, spring, and early summer, whereas f_{SOV} was low during fall and early winter. The measurements in January showed large variability, ranging from the fall group two of the years of measurements to the spring group (one year), thus indicating an interannual variability in the seasonal onset of the intensified transport from the overworld.

[40] The f_{SOV} estimates were related to the measurements of particulate sulfur. Evidence of a discontinuity at the tropopause was found in the average particulate sulfur concentration, being 16 ng/m^3 STP in the tropospheric and 24 ng/m^3 STP in the stratospheric limit. A cause for the step in concentration could be the oxidation of sulfur dioxide, which was transported across the tropopause along with the particles, to form sulfate aerosol in the prolonged residence time since passage through the tropopause. The particulate sulfur concentration increases with f_{SOV} and reaches on average 75 ng/m^3 STP for $f_{\text{SOV}} = 1$. This is the estimated concentration without any influence from the troposphere, hence reflecting the concentration at the top of the lowermost stratosphere.

[41] This strong increase with altitude in the STP concentration (mixing ratio) of particulate sulfur in the lowermost stratosphere connects to the stratospheric overworld. Satellite and balloon-based measurements show further increase of the STP aerosol concentration with altitude. This gradient appears as a result of mixing of down-welling midlatitude air masses with air masses from the tropical stratosphere that are poor in sulfate aerosol mass and active sulfate precursors. As the diabatic flux reaches the lowermost stratosphere, further dilution of the particulate sulfur content results from mixing with tropospheric air on the way down to the tropopause.

[42] The concentration at the top of the lowermost stratosphere was used together with the concentration of sulfur species from the tropical troposphere to estimate that approximately half of the particulate sulfur mass transported from the stratospheric overworld to the lowermost stratosphere was formed from carbonyl sulfide (OCS), the remainder being dominated by particulate sulfur and sulfur dioxide that was transported across the tropical tropopause. The results were further used to estimate the production of particulate sulfur in the stratosphere to 0.066 Tg S/yr . Recent budget estimates arrived at 0.060 , 0.067 , and 0.21 Tg S/yr .

[43] The influence from non-OCS sources becomes stronger in the lowermost stratosphere due to transport of particulate sulfur and sulfur dioxide from the troposphere across the extratropical tropopause. The stratospheric measurements of this study were on average taken at 254 hPa atmospheric pressure with the average PV of 5.4 PVU . The average contribution from the stratospheric overworld was estimated at 40% in terms of air mass and on average two thirds of the particulate sulfur originated in the stratospheric overworld. The particulate sulfur at this level in the lowermost stratosphere thus is made up of three sources of

approximately equal importance: the OCS contribution, the particulate sulfur and sulfur dioxide transported across the tropical tropopause, and the same constituents transported across the extratropical tropopause.

Appendix A: O₃-Based Model on the Air Origin

[44] The long chemical lifetime of ozone of more than 1 year in the midlatitude lowermost stratosphere [Solomon *et al.*, 1997; Smith *et al.*, 2001] was utilized to estimate the fraction of the air in the lowermost stratosphere originating in the overworld. A simple model was formulated. It takes its starting point at the upper bound of the lowermost stratosphere. As the air descends farther into the lowermost stratosphere, the O₃ concentration is reduced mainly as a result of mixing with air of tropospheric origin. Thus the measured O₃ concentration can be described by

$$C_{\text{meas}} = f_{\text{SOV}}C_{\text{SOV}} + (1 - f_{\text{SOV}})C_T, \quad (\text{A1})$$

where f_{SOV} is the sought fraction of air from the stratospheric overworld, whereas C_{SOV} and C_T are the O₃ concentrations at the lower bound of the stratospheric overworld and the troposphere obtained after integration with suitable time constants.

[45] The O₃ concentration at the measurement altitude is the result of mixing of air masses having resided for various time periods in the lowermost stratosphere after they have been transported either across the top of the lowermost stratosphere or the tropopause. The distribution of air mass ages present basically is determined by the air residence time in the lowermost stratosphere. To obtain the O₃ concentrations from the two boundaries (C_{SOV} and C_T), the momentary concentrations at the two boundaries need to be integrated backward in time. The range of momentary concentrations affecting the lowermost stratosphere is determined by the air residence time. The chemical lifetime is also involved in the integrations and produces a correction for chemical loss of O₃.

A1. Model Input Parameters

[46] In situ measurements of O₃ in the upper troposphere have been undertaken by the CARIBIC and MOZAIC [Marenco *et al.*, 1998] platforms. Their monthly mean concentrations, as presented by Zahn *et al.* [2002], were used to obtain concentrations needed to estimate C_T .

[47] The O₃ concentration at the top of the lowermost stratosphere was estimated from ozonesonde data taken at four stations between 38°N and 74°N [Fortuin and Kelder, 1998], where the O₃ concentrations were given as a function of atmospheric pressure. The upper limit of the lowermost stratosphere mostly is described in terms of a potential temperature surface, commonly 380 K . The pressure increases by approximately 15 hPa from 40°N to 60°N on the 380-K surface [Appenzeller *et al.*, 1996]. The latitude dependence of annual average concentrations was fitted to a linear model using 130 hPa concentrations at 40°N and 145 hPa at 60°N . The seasonal variation of the O₃ concentration was close to sinusoidal with a small latitude-dependent phase shift ($O(\Theta)$). The amplitude (A) of the seasonal variation showed small, but irregular variation and was therefore taken to be independent of latitude in the

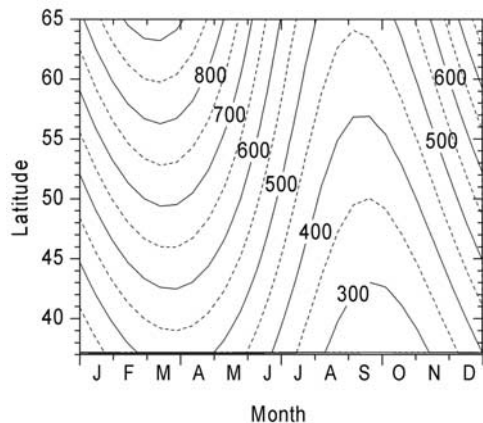


Figure A1. Ozone concentrations (ppbv) used to describe the conditions at the top of the lowermost stratosphere defined by the potential temperature 380 K. The concentrations were extracted from *Fortuin and Kelder* [1998]. See the text for further details.

model. The latitude and season dependent O_3 concentration at the potential temperature 380 K for northern midlatitudes thus was described by

$$C_{SOV}(\Theta, D) = C_0(\Theta) \left[1 + A \sin \left(2\pi \frac{D + O(\Theta)}{365} \right) \right], \quad (A2)$$

where Θ is latitude, D is the Julian day and C_0 is the latitude-dependent, annual average O_3 concentration. The resulting O_3 concentration at the top of the lowermost stratosphere used in the model is shown in Figure A1.

[48] The lowermost stratosphere is ventilated by transport to the troposphere. This stratosphere to troposphere transport (STT) determines the residence time of air in the lowermost stratosphere and hence the integration time constant of C_{SOV} and C_T making up the O_3 concentration. Estimates of STT vary significantly and are method dependent [*Gettelman and Sobel*, 2000]. *Stohl* [2001] estimated the annual average STT to be in the range of 15×10^9 to 35×10^9 kg s^{-1} for the Northern Hemisphere, depending

on the PV depth of the tropopause. Making the assumption that the residence time of air can be approximated by its average value in the stable structure of the lowermost stratosphere and using a value of the STT in the range of *Stohl's* [2001] in relation to the mass of the northern lowermost stratosphere [*Appenzeller et al.*, 1996] yields an average residence time in the range of 2.5–6 months. In the present model, the residence time of air in the lowermost stratosphere was set to 4 months.

A2. Sensitivity Study

[49] The two linear models on the $f_{SOV} - PV$ and $C_{S, strat} - f_{SOV}$ relations shown in Figures 6 and 7 describe in a reduced form the outputs of the O_3 -based model presented here. Hence the sensitivity of these linear models to changes in the input parameters of the O_3 -based model was used to test the stability of the results. Each of the two linear relations was investigated in two points. The $f_{SOV} - PV$ relation was checked for the PV where $f_{SOV} = 0$, which can be regarded as the average PV of the tropopause, and f_{SOV} at PV = 10 PVU. The other relation was investigated with respect to the particulate sulfur concentration ($C_{S, strat}$) for f_{SOV} of 0 and 1. The values at these four points are given in Table A1 together with the 95% probability range of the linear models; for example, the PV of the dynamical tropopause on average is 1.79 PVU and the 95% confidence interval of that estimate 1.21–2.21 PVU.

[50] The mixing of air masses of various ages in the lowermost stratosphere was described using the residence time of air in the lowermost stratosphere. Typical O_3 concentrations of air from the two borders of the lowermost stratosphere were obtained from integration in time. O_3 destruction was accounted for by the inclusion of the chemical lifetime in the model. The central value and test range of the residence time and chemical lifetime were 4 months (2.5–6 months) and 18 ± 6 months. In Table A1 it can be seen that the large range in the air residence time of more than a factor 2 affected the four parameters investigated by $\pm 7\%$ or less. A slightly larger effect was found when the O_3 lifetime was reduced to 12 months on $C_{S, strat}(0)$, which was reduced by 10%, whereas the other parameters were affected by $\pm 7\%$ or less. Comparing with the statistical uncertainty of the estimates, only $f_{SOV}(10)$ is

Table A1. Sensitivity Test of the O_3 -Based Model on the Origin of the Air in the Lowermost Stratosphere

Parameter ^a	Sensitivity Test ^a	$C_S(0)$, ^b ng/m ³ STP	$C_S(1)$, ^b ng/m ³ STP	PV, ^c PVU	$f_{SOV}(10)$ ^d
Model central value ^c	...	8.3	75.2	1.79	0.98
Model 95% statistical interval ^c	...	−0.8–17.4	59.4–90.9	1.21–2.21	0.89–1.05
τ_{O_3} (18 months) ^f	12; 24	7.5–8.7	72.5–76.6	1.71–1.84	1.05–0.94
τ_{air} (4 months) ^g	2.5; 6	8.0–8.5	80.6–71.5	1.87–1.76	0.90–1.04
C_{O_3} annual average (C_0) ^h	$0.9C_0$; $1.1C_0$	8.1–8.5	69.9–80.4	1.79–1.80	1.10–0.88
C_{O_3} amplitude (0.34) ^h	0.306; 0.374	8.5–8.1	74.5–75.8	1.80–1.79	0.98–0.97
C_{O_3} phase (Θ months) ^h	± 0.5	8.5–8.3	73.8–75.8	1.74–1.85	0.98–0.98
Transport delay (0 months) ⁱ	1	8.8	69.4	1.70	1.06
Range in sensitivity test	...	7.5–8.8	69.4–80.6	1.70–1.87	0.88–1.10

^aThe central values of the parameters are given in parentheses. The same units apply to the sensitivity test.

^bParticulate sulfur concentration for f_{SOV} 0 and 1.

^cPotential vorticity for $f_{SOV} = 0$.

^dFraction air from stratospheric overworld at 10 PVU potential vorticity.

^eCentral values and 95% confidence intervals of the linear models in Figures 6 and 7.

^fChemical lifetime of O_3 in the lowermost stratosphere.

^gThe residence time of air in the lowermost stratosphere.

^hThe O_3 concentration at top of the lowermost stratosphere is described by equation (A2).

ⁱTransport delay before air from top of the lowermost stratosphere starts to appear at measurement altitude.

affected to a degree comparable with the statistical uncertainty of the linear model.

[51] Three of the tested input parameters of the O₃-based model concerned the O₃ concentration at the top of the lowermost stratosphere. The interannual, monthly standard deviation at northern midlatitudes is dependent on altitude, latitude, and season. At the top of the lowermost stratosphere at northern midlatitudes the standard deviation typically is in the range of 20–30% [Fortuin and Kelder, 1998]. Their data were, however, based on a large number of years, implying that most of this variability should be accounted for by their averages. Still, to test the O₃ model sensitivity to uncertainties in the average, the annual average was varied by ±10%, as was the amplitude of the seasonal variation, whereas seasonal dependence was shifted by ±0.5 months. The latter two parameters only have a weak influence, 3% or less, on the four points tested (see Table A1). Changing the annual average O₃ concentration by ±10% had little effect on $C_{S, \text{strat}}(0)$ and $PV(f_{\text{SOV}} = 0)$, ±3% or less, whereas $C_{S, \text{strat}}(1)$ changed by ±7% and $f_{\text{SOV}}(10)$ changed by −10% or +13%. Only $f_{\text{SOV}}(10)$ showed sensitivity comparable with the statistical ranges.

[52] Obviously some transport time is required before air at the top of the lowermost stratosphere starts to appear at the measurement altitudes. Ozone-sonde data presented by Fortuin and Kelder [1998] show that the early spring maximum at northern midlatitudes appears in the same month at the top of the lowermost stratosphere and at pressures of above 200 hPa at four stations in the range 38–74°N. On the basis of this observation the delay time before the air masses appear at our measurement altitudes was set to 0; that is, the starting time of the integration backwards in time to obtain C_{SOV} was set to the time of the measurement as the model central value. The sensitivity to this transport time was tested by a delay of 1 month; that is, the backward integration started 1 month before the time of observation. In Table A1 it can be seen that the deviation from the central value was 8% or less, which is small compared with the statistical ranges for all testing points except for $f_{\text{SOV}}(10)$.

[53] The influence of the interannual, monthly standard deviation was tested by changing the O₃ concentration by ±25% during the most recent month of each measurement, whereas the concentration followed the average behavior the preceding months. This test is somewhat unrealistic when applied to the parameters of Table A1, because all samples, taken during a 3-year period, are affected in the same direction (±25%) by the test. However, this estimate can be used to test the behavior of individual measurements. On average, f_{SOV} over all the stratospheric model layers was 0.395. Increase of the O₃ concentration by 25% decreased the average f_{SOV} by 7.7% and became 0.365, whereas the 25% decrease in O₃ increased average f_{SOV} by 9.1%. These numbers thus can be regarded as an estimate on the variability in f_{SOV} induced by the interannual variability in the O₃ concentration at top of the lowermost stratosphere.

[54] In conclusion, it was found that the O₃-based model constitutes a robust tool to estimate the particulate sulfur concentration at the tropopause and the top of the lowermost stratosphere. This is also true for the average position in PV of the tropopause, whereas the fraction of air from the lowermost stratosphere at $PV = 10$ PVU showed sensitivity

to estimated values used in the model that were similar to the statistical uncertainties of the linear model used.

[55] **Acknowledgments.** The collaboration with LTU International Airways, Düsseldorf, Germany, providing an aircraft modified for the CARIBIC sampling, is gratefully acknowledged. The work was supported financially by the European Union, the Swedish Research Council, and the Swedish Environment Protection Agency (research grants ENV-CT95-0006, EKV2-CT-2001-00101, 621-2002-5331, and 011-121-98-01).

References

- Appenzeller, C., J. R. Holton, and K. H. Rosenlof (1996), Seasonal variation of mass transport across the tropopause, *J. Geophys. Res.*, *101*, 15,071–15,078.
- Arnold, F., J. Curtis, S. Spreng, and T. Deshler (1998), Stratospheric aerosol sulfuric acid: First direct in situ measurements using a novel balloon-based mass spectrometer apparatus, *J. Atmos. Chem.*, *30*, 3–10.
- Bauman, J. J., P. B. Russell, M. A. Geller, and P. Hamill (2003), A stratospheric aerosol climatology from SAGE II and CLAES measurements: 2. Results and comparisons, 1984–1999, *J. Geophys. Res.*, *108*(D13), 4383, doi:10.1029/2002JD002993.
- Brenninkmeijer, C. A. M., et al. (1999), CARIBIC—Civil aircraft for global measurement of trace gases and aerosols in the tropopause region, *J. Atmos. Oceanic Technol.*, *16*, 1373–1383.
- Brewer, A. W. (1949), Evidence for a world circulation provided by the measurements of helium and water vapour distribution in the stratosphere, *Q. J. R. Meteorol. Soc.*, *75*, 351–363.
- Brock, C. A., P. Hamill, J. C. Wilson, H. H. Jonsson, and K. R. Chan (1995), Particle formation in the upper tropical troposphere: A source of nuclei for the stratospheric aerosol, *Science*, *270*, 1650–1653.
- Chin, M., and D. D. Davies (1995), A reanalysis of carbonyl sulfide as a source of stratospheric background sulfur aerosol, *J. Geophys. Res.*, *100*, 8993–9005.
- Crutzen, P. J. (1976), The possible importance of OCS for the sulfate layer of the stratosphere, *Geophys. Res. Lett.*, *3*, 73–76.
- Danielsen, E. F. (1968), Stratospheric-tropospheric exchange based upon radioactivity, ozone and potential vorticity, *J. Atmos. Sci.*, *25*, 502–518.
- Deshler, T., M. E. Hervig, D. J. Hofmann, J. M. Rosen, and J. B. Liley (2003), Thirty years of in situ stratospheric aerosol size measurements from Laramie, Wyoming (41°N), using balloon-borne instruments, *J. Geophys. Res.*, *108*(D5), 4167, doi:10.1029/2002JD002514.
- Dessler, A. E., E. J. Hints, E. M. Weinstock, J. G. Anderson, and K. R. Chan (1995), Mechanisms controlling water vapor in the lower stratosphere: “A tale of two stratospheres,” *J. Geophys. Res.*, *100*(D11), 23,167–23,172.
- Dobson, G. M. B. (1956), Origin and distribution of polyatomic molecules in the atmosphere, *Proc. R. Soc. London, Ser. A*, *236*, 187–193.
- Fortuin, J. P. F., and H. Kelder (1998), An ozone climatology based on ozone-sonde and satellite measurements, *J. Geophys. Res.*, *103*(D24), 31,709–31,734.
- Gettelman, A., and A. H. Sobel (2000), Direct diagnoses of stratosphere-troposphere exchange, *J. Atmos. Sci.*, *57*, 3–16.
- Gettelman, A., J. R. Holton, and K. H. Rosenlof (1997), Mass fluxes of O₃, CH₄, N₂O, and CF₂Cl₂ in the lower stratosphere calculated from observational data, *J. Geophys. Res.*, *102*(D15), 19,149–19,159.
- Hermann, M., F. Stratmann, M. Wilck, and A. Wiedensohler (2001), Sampling characteristics of an aircraft-borne aerosol inlet system, *J. Atmos. Oceanic Technol.*, *18*, 7–19.
- Hermann, M., J. Heintzenberg, A. Wiedensohler, A. Zahn, G. Heinrich, and C. A. M. Brenninkmeijer (2003), Meridional distributions of aerosol particle number concentrations in the upper troposphere and lower stratosphere obtained by Civil Aircraft for Regular Investigation of the Atmosphere Based on an Instrument Container (CARIBIC) flights, *J. Geophys. Res.*, *108*(D3), 4114, doi:10.1029/2001JD001077.
- Hoerling, M. P., T. K. Schaack, and A. J. Lenzen (1991), Global objective tropopause analysis, *Mon. Weather Rev.*, *119*, 1816–1831.
- Hofmann, D. J. (1993), Twenty years of balloon-borne tropospheric aerosol measurements at Laramie, Wyoming, *J. Geophys. Res.*, *98*, 12,753–12,766.
- Hoinka, K. P. (1997), The tropopause: Discovery, definition and demarcation, *Meteorol. Z.*, *6*, 281–303.
- Holton, J. R., P. H. Haynes, M. E. McIntyre, A. R. Douglass, R. B. Rood, and L. Pfister (1995), Stratosphere-troposphere exchange, *Rev. Geophys.*, *33*, 403–439.
- Hoor, P., H. Fischer, L. Lange, J. Liliieveld, and D. Brunner (2002), Seasonal variations of a mixing layer in the lowermost stratosphere as identified by the CO-O₃ correlation from in situ measurements, *J. Geophys. Res.*, *107*(D5), 4044, doi:10.1029/2000JD000289.

- Hoskins, B. J. (1991), Towards a PV-theta view of the general circulation, *Tellus, Ser. AB*, 43, 27–35.
- Intergovernmental Panel on Climate Change (2001), Climate change 2001—The scientific basis: Contribution of Working Group I to the Third Assessment Report of the Intergovernmental Panel on Climate Change, edited by J. T. Houghton et al., pp. 289–348, Cambridge Univ. Press, New York.
- James, P., A. Stohl, C. Forster, S. Eckhardt, P. Seibert, and A. Frank (2003), A 15-year climatology of stratosphere-troposphere exchange with a Lagrangian particle dispersion model: 2. Mean climate and seasonal variability, *J. Geophys. Res.*, 108(D12), 8522, doi:10.1029/2002JD002639.
- Johansson, S. A. E., and J. L. Campbell (1988), *PIXE: A Novel Technique for Elemental Analysis*, John Wiley, Hoboken, N. J.
- Junge, C. E., C. W. Chagnon, and J. E. Manson (1961), Stratospheric aerosols, *J. Meteorol.*, 18, 81–108.
- Kent, G. S., P.-H. Wang, M. P. McCormick, and K. M. Skeens (1995), Multiyear Stratospheric Aerosol and Gas Experiment II measurements of upper tropospheric aerosol characteristics, *J. Geophys. Res.*, 100, 13,875–13,899.
- Kjellström, E. (1998), A three-dimensional global model study of carbonyl sulfide in the troposphere and the lower stratosphere, *J. Atmos. Chem.*, 29, 151–177.
- Liley, J. B., J. M. Rosen, N. T. Kjome, N. B. Jones, and C. P. Rinsland (2001), Springtime enhancement of upper tropospheric aerosol at 45°S, *Geophys. Res. Lett.*, 28, 1495–1498.
- Marenco, A., et al. (1998), Measurement of ozone and water vapor Airbus in-service aircraft: The MOZAIC airborne program, An overview, *J. Geophys. Res.*, 103(D19), 25,631–25,642.
- Martinsson, B. G., G. Papaspiropoulos, J. Heintzenberg, and M. Hermann (2001), Fine mode particulate sulphur in the tropopause region measured from intercontinental flights (CARIBIC), *Geophys. Res. Lett.*, 28, 1175–1178.
- Newman, P. A., et al. (2002), An overview of the SOLVE/THESEO 2000 campaign, *J. Geophys. Res.*, 107(D20), 8259, doi:10.1029/2001JD001303.
- Papaspiropoulos, G., B. Mentes, P. Kristiansson, and B. G. Martinsson (1999), A high sensitivity elemental analysis methodology for upper tropospheric aerosol, *Nucl. Instrum. Methods, B150*, 356–362.
- Papaspiropoulos, G., B. G. Martinsson, A. Zahn, C. A. M. Brenninkmeijer, M. Hermann, J. Heintzenberg, H. Fischer, and P. F. J. van Velthoven (2002), Aerosol elemental concentrations in the tropopause region from intercontinental flights with the Civil Aircraft for Regular Investigation of the Atmosphere Based on an Instrument Container (CARIBIC) platform, *J. Geophys. Res.*, 107(D23), 4671, doi:10.1029/2002JD002344.
- Rasch, et al. (2000), A comparison of scavenging and deposition processes in global models: Results from the WCRP Cambridge workshop 1995, *Tellus, Ser. B*, 52, 1025–1056.
- Roelofs, G. J., and J. Lelieveld (2000), Model analysis of stratosphere-troposphere exchange of ozone and its role in the tropospheric ozone budget, in *Chemistry and Radiation Changes in the Ozone Layer*, edited by C. S. Zerefos et al., pp. 25–43, Springer, New York.
- Rosen, J. M. (1971), The boiling point of stratospheric aerosols, *J. Appl. Meteorol.*, 10, 1044–1045.
- Smith, J. B., E. J. Hints, N. T. Allen, R. M. Stimpfle, and J. G. Anderson (2001), Mechanisms for midlatitude ozone loss: Heterogeneous chemistry in the lowermost stratosphere?, *J. Geophys. Res.*, 106(D1), 1297–1309.
- Solomon, S., S. Borrmann, R. R. Garcia, R. Portmann, L. Thomason, L. R. Poole, D. Winkler, and P. McCormick (1997), Heterogeneous chlorine chemistry in the tropopause region, *J. Geophys. Res.*, 102(D17), 21,411–21,429.
- Sprenger, M., and H. Wernli (2003), A northern hemispheric climatology of cross-tropopause exchange for the ERA 15 time period (1979–1993), *J. Geophys. Res.*, 108(D12), 8521, doi:10.1029/2002JD002636.
- Stohl, A. (2001), A 1-year Lagrangian “climatology” of airstreams in the Northern Hemisphere troposphere and lowermost stratosphere, *J. Geophys. Res.*, 106, 7263–7279.
- Stohl, A., et al. (2003), Stratosphere-troposphere exchange: A review, and what we have learned from STACCATO, *J. Geophys. Res.*, 108(D12), 8516, doi:10.1029/2002JD002490.
- Takigawa, M., M. Takahashi, and H. Akiyoshi (2002), Simulation of stratospheric sulfate aerosols using a Center for Climate System Research/National Institute for Environmental Studies atmospheric GCM with coupled chemistry: 1. Nonvolcanic simulation, *J. Geophys. Res.*, 107(D22), 4610, doi:10.1029/2001JD001007.
- Thornton, D. C., A. R. Bandy, B. W. Blomquist, A. R. Driedger, and T. P. Wade (1999), Sulfur dioxide distribution over the Pacific Ocean 1991–1996, *J. Geophys. Res.*, 104, 5845–5854.
- Weisenstein, D. K., G. K. Yue, M. K. W. Ko, N.-D. Sze, J. M. Rodriguez, and C. J. Scott (1997), A two-dimensional model of sulfur species and aerosols, *J. Geophys. Res.*, 102, 13,019–13,035.
- Zahn, A., C. A. M. Brenninkmeijer, W. A. H. Asman, P. J. Crutzen, G. Heinrich, H. Fischer, J. W. M. Cuijpers, and P. F. J. van Velthoven (2002), Budgets of O₃ and CO in the upper troposphere: The CARIBIC passenger aircraft results 1997–2001, *J. Geophys. Res.*, 107(D17), 4337, doi:10.1029/2001JD001529.
- Zahn, A., C. A. M. Brenninkmeijer, and P. F. J. van Velthoven (2004a), Passenger aircraft project CARIBIC 1997–2002: Part I. The extratropical chemical tropopause, *Atmos. Chem. Phys. Discuss.*, 4, 1091–1117.
- Zahn, A., C. A. M. Brenninkmeijer, and P. F. J. van Velthoven (2004b), Passenger aircraft project CARIBIC 1997–2002: Part II. The ventilation of the lowermost stratosphere, *Atmos. Chem. Phys. Discuss.*, 4, 1119–1150.
- Zuev, V. V., V. D. Burlakov, A. V. El'nikov, A. P. Ivanov, A. P. Chaikovskii, and V. N. Shcherbakov (2001), Processes of long-term relaxation of stratospheric aerosol layer in Northern Hemisphere midlatitudes after a powerful volcanic eruption, *Atmos. Environ.*, 35, 5059–5066.

C. A. M. Brenninkmeijer, Division of Atmospheric Chemistry, Max Planck Institute for Chemistry, P.O. Box 3060, D-55020 Mainz, Germany. J. Heintzenberg and M. Hermann, Leibniz-Institute for Tropospheric Research, Permoserstrasse 15, D-04318 Leipzig, Germany.

B. G. Martinsson and H. N. Nguyen, Division of Nuclear Physics, Lund University, P.O. Box 118, S-22100 Lund, Sweden. (bengt.martinsson@nuclear.lu.se)

P. F. J. van Velthoven, Atmospheric Composition Research, Royal Netherlands Meteorological Institute (KNMI), P.O. Box 201, 3730 AE De Bilt, Utrecht, Netherlands.

A. Zahn, Institute of Meteorology and Climate Research, Forschungszentrum Karlsruhe, P.O. Box 3640, D-76021 Karlsruhe, Germany.